

## 몰리브데늄 옥소 알콕소 문치 화합물의 합성과 분자 구조 및 졸-겔 법에 의한 자기저항 산화물제조

金正泳 · 李甫和 · 河炫俊 · 蔡熙權\*

한국외국어대학교 화학과

한국외국어대학교 전자물리학과

(2001. 5. 11 접수)

## Synthesis and Molecular Structure of An Octanuclear Oxomolybdenum(V) Cluster Compound and Its Sol-Gel Application to Magneto-resistant Oxides

Jung Young Kim, Bo Wha Lee<sup>†</sup>, Hyun-Joon Ha, and Hee K. Chae\*

Department of Chemistry, Hankuk University of Foreign Studies, Yongin 449-791, Korea

<sup>†</sup>Department of Electronic Physics, Hankuk University of Foreign Studies, Yongin 449-791, Korea

(Received May 11, 2001)

The colossal magnetoresistance (CMR) in perovskite oxides including doped manganates<sup>1</sup> has attracted great attention. But it is questionable whether these compounds would be useful for most applications, because the high values of magnetoresistance (MR) only occur with magnetic fields as high as 7 T and or temperatures as low as 5 K. Recently, the ordered double perovskite  $\text{Sr}_2\text{FeMoO}_6$  has been reported to have a low-field MR at room temperature (RT) and a high Curie temperature over 400 K.<sup>2</sup> The large MR, however, can be obtained only in high magnetic fields of several Tesla at RT. For magnetic recording devices, magnetic materials should have a large MR at low fields and ambient temperatures. The sol-gel process is one of the candidate methods used to enhance the low field MR of  $\text{Sr}_2\text{FeMoO}_6$  because of relatively easy control of particle size with high purity and homogeneous stoichiometry.<sup>3</sup> Even though a limited number of the sol-gel methods are reported for the preparation of mixed-metal perovskite magnetic oxides, the study of the alkoxide or oxoalkoxide precursors to  $\text{Sr}_2\text{FeMoO}_6$  remains relatively unexplored.<sup>4</sup> Here, we demonstrate the preparation and structural characterization of an octamolybdenum(V) oxoalkoxide precursor, and its application to low-field, RT, high MR and poly-

crystalline  $\text{Sr}_2\text{FeMoO}_6$  by sol-gel process.

The molybdenum precursor complex was obtained from  $\text{Mo}(\text{O})\text{Cl}_5$ <sup>5</sup> and the potassium salt of triethanolamine in methanol. The synthetic procedure yielded single crystals of  $[\text{Mo}_8(\text{O})_8(\mu_3\text{-O})_2(\mu_2\text{-O})_6(\mu_2\text{-OCH}_3)_2(\mu_2\text{-OCH}_3)_4\text{Cl}_2(\text{HOCH}_2)_4 \cdot 6(\text{CH}_3\text{OH})]$  (1).<sup>6</sup> X-ray characterization was performed to reveal the solid state structure depicted in Fig. 1. The crystallographic analysis shows the presence of a neutral  $\text{Mo}(\text{V})$  complex in which four  $\text{Mo}^{\text{V}}(\text{O})(\mu_3\text{-O})(\mu_2\text{-O})(\mu_2\text{-OCH}_3)\text{-Mo}^{\text{V}}(\text{O})(\mu_3\text{-O})(\mu_2\text{-O})(\mu_2\text{-OCH}_3)$  dimers are bound to share edges each other. Each molybdenum atom has one solvated methanol and or one chlo-

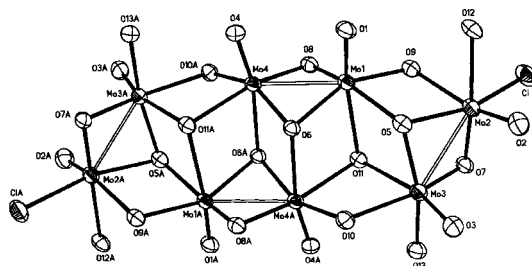


Fig. 1. ORTEP drawing of  $[\text{Mo}_8(\text{O})_8(\mu_3\text{-O})_2(\mu_2\text{-O})_6\text{Cl}_2]\text{core}$  of  $[\text{Mo}_8(\text{O})_8(\mu_3\text{-O})_2(\mu_2\text{-O})_6(\mu_2\text{-OCH}_3)_2(\mu_2\text{-OCH}_3)_4\text{Cl}_2(\text{HOCH}_2)_4 \cdot 6(\text{CH}_3\text{OH})]$  (1).

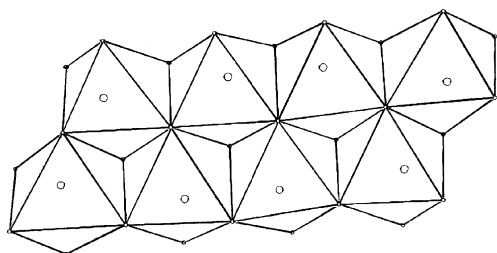


Fig. 2. Polyhedral representation drawing of  $[\text{Mo}_4(\text{O})_2(\mu_2\text{-O})_2(\mu_2\text{-OCH}_3)_2\text{Cl}_2]$  core of  $[\text{Mo}_8(\text{O})_6(\mu_2\text{-O})_4(\mu_2\text{-O})_2(\mu_2\text{-OCH}_3)_2(\mu_2\text{-OCH}_3)_2\text{Cl}_2(\text{HOCH}_3)_4 \cdot 6(\text{CH}_3\text{OH})]$  (**1**).

ride. In Fig. 2 two chains of four octahedra Mo are fused to form a chain structure, which is similar to chains of  $\text{MoO}_3(\text{OH}_2)$  octahedra in the structure of  $\alpha\text{-MoO}_3 \cdot \text{H}_2\text{O}$ . Addition of base to  $[\text{MoOCl}_4]^{2-}$  yields a brown precipitate that is often formulated as  $[\text{MoO}(\text{OH})_2]$  but no structural information is available for this substance or any  $[\text{Mo}_2\text{O}_7]$  species, even though mixed-valence oxides are well-characterized crystallographically including rhombohedral and monoclinic phases of  $\text{Mo}_8\text{O}_{23}$  ( $7\text{MoO}_3 \cdot \text{MoO}_2$ ).<sup>20</sup> Thus, **1** may provide useful information about pure "Mo(V) oxide" phases.

In the core of the  $[\text{Mo}_4\text{O}_{10}]^{12+}$  moiety of **1**, the coordination around the molybdenum ion has one terminal oxo, one  $\mu_2\text{-O}$ , one  $\mu_2\text{-OCH}_3$ , three  $\mu_2\text{-O}$  and Mo-Mo bond (2.5782 Å average distance) (see Table 1 and Fig. 3). The tetranuclear core cluster is a well-known structural motif in the coordination chemistry of polyoxomolybdates, especially Mo(VI) complexes. The most frequently encountered arrangement is exemplified by the cluster  $[\text{Mo}_4\text{O}_{10}(\text{OMe})_4]^{2-}$ , which possesses four edge-sharing octahedra.<sup>7</sup> Each molybdenum ion in the structure of  $[\text{Mo}_4\text{O}_{10}(\text{OMe})_4]^{2-}$  coordinates to one terminal  $\text{OCH}_3$ , one  $\mu_2\text{-O}$ ,

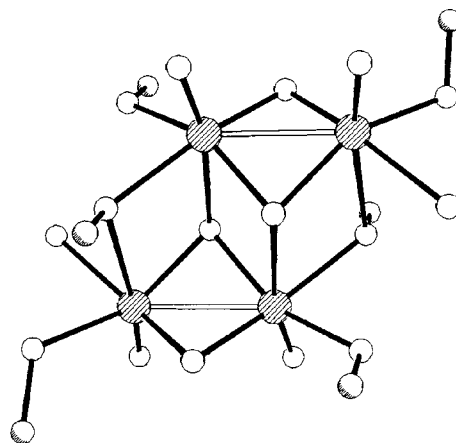


Fig. 3. Ball and stick drawing of  $[\text{Mo}_4(\text{O})_2(\mu_2\text{-O})_2(\mu_2\text{-O})_2(\mu_2\text{-OCH}_3)_2(\text{OCH}_3)_2]$  core of  $[\text{Mo}_8(\text{O})_6(\mu_2\text{-O})_4(\mu_2\text{-O})_2(\mu_2\text{-OCH}_3)_2(\mu_2\text{-OCH}_3)_2\text{Cl}_2(\text{HOCH}_3)_4 \cdot 6(\text{CH}_3\text{OH})]$  (**1**).

$\text{OCH}_3$ , one  $\mu_2\text{-O}$ , one  $\mu_2\text{-OCH}_3$ , and two terminal oxo oxygens. The alkoxy ligands can substitute a number of oxo groups to reduce the charge and stabilize the cluster in alcoholic solvents. This provides the basis for a number of Mo(VI) species including  $[\text{Mo}_4\text{O}_{10}(\text{OMe})_4\text{Cl}_2]^{2-}$  and  $[\text{Mo}_4\text{O}_{10}(\text{OEt})_2(\text{OCH}_2\text{CR})_2]^{2-}$ . The Mo(VI) cluster,  $[\text{Mo}_4\text{O}_{10}(\text{OMe})_4\text{Cl}_2]^{2-}$  may be reduced into analogue Mo(V) species,  $[\text{Mo}_4\text{O}_{10}(\text{OMe})_2(\text{MeOH})_2\text{Cl}_2]^{2-}$ , whose core structure is isostructural to the tetranuclear core of **1**, as shown in Fig. 3. Limberg and coworkers have reported structure and characterization of oxomolybdenum(V) clusters from the reaction between  $\text{MoCl}_5$  and alcohols.<sup>8</sup> Molecular structures of  $[\text{Mo}_4\text{O}_{10}\text{Cl}_2(\mu_2\text{-OEt})(\text{PMe}_2)_2(\mu_2\text{-O})_2]$  (**2**)<sup>8c</sup> and  $[\text{Mo}_4\text{O}_{10}(\mu_2\text{-O})_2(\mu_2\text{-O})_2(\mu_2\text{-OH})_2][\text{Hpz}^{\text{Me}_2}]_2^{2-}$  ( $\text{Hpz}^{\text{Me}_2} = 3,5\text{-dimethylpyrazole}$ ) (**3**)<sup>8</sup> also show  $\text{Mo}_4$  core clusters similar with that of **1**. Sometimes the partial reduction of Mo(VI) to Mo(V) produces mixed-valence Mo(V)/Mo(VI) species including  $[\text{Mo}_4\text{O}_{10}(\text{OPr})(\text{PrOH})_2\text{Cl}_2]^{10}$ .

As far as we know, the structure of **1** is unique. There are a number of octanuclear molybdate species in polyoxomolybdates,<sup>7</sup> based on the  $\beta$ -molybdate(VI),  $[\text{Mo}_8\text{O}_{23}]^{8-}$  structure including  $[\text{Mo}_8\text{O}_{23}(\text{OMe})_4]^{4-}$ ,  $[\text{Mo}_8\text{O}_{23}(\text{HCO}_2)_2]^{6-}$  and  $[\text{Mo}_8\text{O}_{23}(\text{sal})_2]^{2-}$  (sal=salicylidenepropyliminato). Relatively few examples of Mo(V) clusters are known:<sup>7</sup>  $[\text{Mo}_8\text{O}_{23}(\text{OMe})_4(\text{C}_2\text{O})_4]^{4-}$ ,  $[\text{Mo}_8\text{O}_{23}(\text{OMe})_4(\text{PR}_3)_4]$  and  $[\text{Mo}_8\text{O}_{23}\text{Cl}_2(\mu_2\text{-O})_4(\text{OH})_2(\mu_2\text{-OH})_2(\mu_2\text{-O})_2(\mu_2\text{-OEt})_2][\text{HOEt}]_2^{11}$  (**4**).<sup>8b,c</sup> The first two clusters exhibit the cyclic framework, while the last one shows the cubane-like distorted rutile struc-

Table 1. Characteristic Average Bond Distances (Å) in the  $\text{Mo}^{\text{V}}$  Clusters

	2	3	4	1
Mo-Mo	2.6647	2.568	2.647	2.5782
Mo-O	1.664	1.681	1.660	1.675
Mo-O( $\mu_2$ )	na	2.172	na	1.932
Mo-O( $\mu_3$ )	1.985	1.977	2.018	2.009
Mo-OR( $\mu_2$ )	1.989	na	1.991	2.113
Mo-OR( $\mu_3$ ) na	na	na	na	2.282

na=not available

ture. However, the structure of **1** shows an one-dimensional extended framework with six  $\mu_2$ -O coordinations, which is quite different from those of three above complexes. Table 1 shows some characteristic average bond lengths of tetramers (**2** and **3**) and octamers (**1** and **4**).

In addition to crystallographic study, complex **1** was also characterized by FT-IR spectroscopy. The spectrum of **1** is much more complicated than that of methanol between 1000 and 430  $\text{cm}^{-1}$ . The band at 970  $\text{cm}^{-1}$  is assigned to the terminal Mo-O bond.<sup>9,11</sup> Bands are also observed at 717, and 681  $\text{cm}^{-1}$ , that can be attributed to asymmetric Mo-O-Mo and terminal Mo-Cl, respectively. Bands at 550, 519, and 494  $\text{cm}^{-1}$  can be attributed to M-O stretching vibration of Mo-OC(H)<sub>3</sub>. These results are well consistent with the solid-state structure.

Polycrystalline samples of Sr<sub>2</sub>FeMoO<sub>6</sub> were prepared by sol-gel process using strontium 2-methoxyethoxide, iron 2-methoxyethoxide and **1** in a metal-based ratio of 2 : 1 : 1 in 2-methoxyethanol.<sup>12</sup> The hydrolyzed precipitate was calcined at 850 °C in air before the powder was pressed into pellets. Samples A, B, C, and D were sintered at temperatures of 875, 900, 1000, and 1100 in a stream of 5% H<sub>2</sub>/Ar for two hours, respectively. Each polycrystalline phase was confirmed by X-ray powder diffraction pattern. The diffraction peaks are indexed with respect to the cubic symmetry (*Fm3m*) with a slight tetragonal distortion.

Preliminary MR investigations of the sample are shown in Fig. 4. The magnitude of negative MR for sample A with the magnetic field of 0.8 T at 12 and 300 K is as large as 33 and 2.5%, respectively.<sup>13</sup> In the case of metallic sample D, the magnitude of MR is smaller than that of semiconducting sample. Since the field dependent magnetization is almost the same for both metallic and semiconducting samples, the discrepancy in MR is not due to a bulk phenomenon. It is a consequence of grain boundary scattering due to different grain size formed at different sintering temperature. Individual moments are aligned by the external magnetic field and the hopping of the spin-polarized electron between grains is controlled by the external field. Therefore the large MR observed in the semiconducting sample is due to the enhanced inter-grain tunneling by reducing the relative angle of magnetization directions at the grain boundaries.

The financial support from the Korea Research Foun-

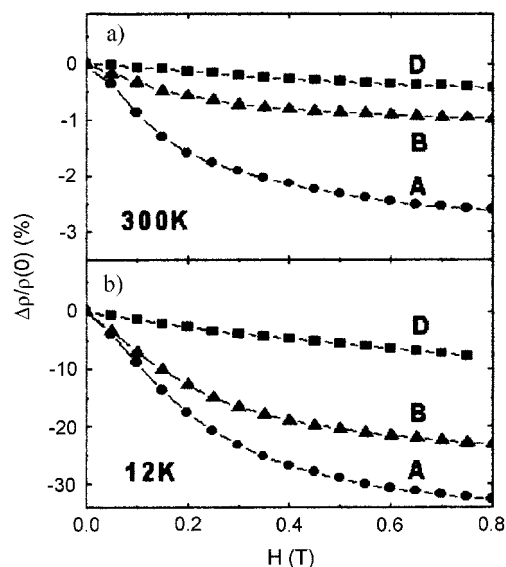


Fig. 4. Magnetoresistance of polycrystalline Sr<sub>2</sub>FeMoO<sub>6</sub> samples for different sintering temperatures.

ation BSRI (1999-015-DP0257) is acknowledged. We are also grateful to Prof. O. M. Yaghi and Dr. Jaheon Kim at University of Michigan for X-ray facilities.

## REFERENCES

- (a) Jin, S.; Tiefel, T. H.; McCormack, M.; Fastnacht, R. A.; Ramesh, R.; Chen, L. H. *Science* **1994**, *264*, 413. (b) *Colossal Magnetoresistance, Charge Ordering and Related Properties of Manganese Oxides*; Rao, C. N. R.; Raveau, B., Ed.; World Scientific: Singapore, 1998.
- Kobayashi, K. I.; Kimura, T.; Sawada, H.; Terakura, K.; Tokura, Y. *Nature* **1998**, *395*, 667.
- (a) Mahía, J.; Vazquez, C.; Mira, J.; Lopez-Quintela, A.; Rivas, J.; Jones, T. E.; Oseroff, S. B. *J. Appl. Phys.* **1994**, *75*, 6757. (b) Yuan, C. L.; Wang, S. G.; Song, W. H.; Yu, T.; Dai, J. M.; Ye, S. L.; Sun, Y. P. *Appl. Phys. Lett.* **1999**, *75*, 3853.
- (a) Chae, H. K.; Hwang, C.; Dong, Y.; Yun, H.; Jang, H. G. *Chem. Lett.* **2000**, 992. (b) Kim, J. Y.; Kim, Y. J.; Park, B. J.; Lee, B. W.; Hwang, C. S.; Choi, C. H.; Chae, H. K.; Kim, C. S. *Molecular Phys. Reports*, in press.
- Larson, M. L.; Moore, F. W. *Inorg. Synth.* **1970**, *12*, 190.
- Addition of the mixture of brown Mo(OCl)<sub>3</sub> (1.00 g, 4.58 mmol) in 100 mL of methanol to the colorless solution of K<sub>2</sub>[(OCH<sub>2</sub>CH<sub>2</sub>)<sub>3</sub>N] (1.20 g, 4.77 mmol) in 50 mL of methanol gave orange crystals of complex

- 1(2.02 g, 1.26 mmol) with 27.5% yield based on molybdenum. IR (KBr pellet,  $\text{cm}^{-1}$ ): 3433(br), 2933(w), 1632(br), 1030(w), 970(s), 717(m), 681(m), 550(m), 519(m), 494(m), 464(w). *Anal.* Found: C, 11.76; H, 3.49; Cl, 4.61. Calc. for  $\text{C}_{16}\text{H}_{18}\text{O}_{12}\text{Cl}_2\text{Mo}_8$ : C, 12.00; H, 3.66; Cl, 4.43. Pink rod-shape crystals of  $[\text{Mo}_8(\text{O})_8(\mu_3\text{-O})_2(\mu_3\text{-O})_2(\mu_3\text{-OCl})_2(\mu_3\text{-OCl})_2)\text{Cl}_2(\text{HOCl})_2 \cdot 6(\text{Cl}_3\text{OI})]$  were analyzed at 208–1 K: triclinic, space group  $P(-1)$  with  $a=7.8373(4)$  Å,  $b=10.1107(5)$  Å,  $c=15.0384(7)$  Å,  $\alpha=92.9500(10)^\circ$ ,  $\beta=98.4170(10)^\circ$ ,  $\gamma=92.2460(10)^\circ$ ,  $V=1175.94(10)$  Å<sup>3</sup>,  $Z=1$ ,  $d_{\text{calc}}=2.261$  g·cm<sup>-3</sup>,  $\mu_0(\text{Mo K}\alpha)=2.263$  mm<sup>-1</sup>, goodness of fit on  $F^2=1.000$ ,  $R=0.0351$  and  $R_w=0.0884$ .
7. (a) Pope, M. T. In *Progress In Inorganic Chemistry*, Lippard, S. J., Ed.: John Wiley & Sons: New York, U. S. A., 1991; Vol. 39, p 181 and references therein. (b) Khan, M. I.; Zubieta, J. In *Progress In Inorganic Chemistry*, Karlin, K. D., Ed.: John Wiley & Sons: New York, U. S. A., 1995; Vol. 43, p 1.
  8. (a) Limberg, C.; Parsons, S.; Downs, A. J.; Wakin, D. *J. Chem. Soc. Dalton Trans.* **1994**, 1169. (b) Blake, A. J.; Parsons, S.; Limberg, C.; Parsons, S. *J. Chem. Soc. Dalton Trans.* **1995**, 3263. (c) Limberg, C.; Downs, A. J.; Blake, A. J.; Parsons, S. *Inorg. Chem.* **1996**, *35*, 4439. (d) Limberg, C.; Boese, R.; Schiemenz, B. *J. Chem. Soc. Dalton Trans.* **1997**, 1633. (e) Limberg, C.; Buchner, M.; Walter, O. *Inorg. Chem.* **1997**, *36*, 872.
  9. Cano, M.; Campo, J. A.; Heras, J. V.; Pinilla, E. *Polyhedron* **1996**, *15*, 1705.
  10. Beaver, J. A.; Drew, M. G. B. *J. Chem. Soc. Dalton Trans.* **1973**, 1376.
  11. Deltecheff, C. R.; Thouvenot, R.; Fouassier, M. *Inorg. Chem.* **1982**, *21*, 30.
  12. Kim, Y.; Chae, H. K.; Lee, K. S.; Lee, W. I. *J. Mater. Chem.* **1998**, *8*, 2317.
  13. The definition of the magnitude of MR:  $\text{MR} = \Delta\rho / \rho(0) = |\rho(H) - \rho(0)| / \rho(0)$  where  $\rho(0)$  is the zero field resistivity and  $\rho(H)$  is the resistivity under magnetic field.